Proceedings of the
47th IEEE Conference on Decision and Control
Cancun, Mexico, Dec. 9-11, 2008

Development of a Flipper Propelled Turtle-like Underwater Robot and Its CPG-based Control Algorithm

Wei Zhao, Yonghui Hu, Long Wang, and Yingmin Jia

Abstract— **This paper presents the construction and control of a turtle-like underwater robot with four mechanical flippers. Each flipper consists of two joints generating a rowing motion by combination of lead-lag and feathering motions. The control architecture is constructed based on central pattern generator (CPG). A model for a system of coupled nonlinear oscillators is established to construct CPG and has been successfully applied to the eight-joint turtle-like robot. The CPGs are modeled as nonlinear oscillators for joints and inter-joint coordination is achieved by altering the connection weights between joints. With cooperative movements of four flippers, the robot can propel and maneuver in any direction without rotation of its main body, and execute complicated 3-D movements including ascending, submerging, rolling, and hovering. The CPG-based method shows elegant and smooth transitions between swimming gaits, and enhanced ability to cope with transient perturbations due to nonlinear characteristic. The effectiveness of the proposed method is confirmed via simulations and experimental results.**

I. INTRODUCTION

Robotics research has shown much progress with the development of robotic technologies to complex and dynamic environments, especially those inaccessible to humans like the outer space and deep oceans. In the fields of ocean development and ocean investigation, various autonomous underwater vehicles (AUVs) have been developed to survey the complex and dynamic undersea environments. However, swimming animals have been evolving their aquatic locomotion abilities for millions of years, surpassing man-made underwater vehicles in many respects such as propulsive efficiency, maneuverability, and acceleration. Based on recent progress in mechanics, material, electronics and bionics, many biologically inspired underwater vehicles that employ biomimetic swimming mechanism have been created to bridge the gap between the mission requirement and available technologies.

In the area of biorobotic AUV, fish-like robot is the early focus and fishlike swimming has become one of interesting research topics. Significant work in robotic fish was initiated in the 1990s by Triantafyllou *et al.* [1], [2]. An eight-link, foil-flapping robotic mechanism, i.e., RoboTuna, was developed and its drag-reduction mechanism was experimentally investigated. With further research on underwater biorobotics, other animals with rowing or flapping appendages such as turtles and penguins are receiving more and more attention. Their paired appendages are used for propulsion and maneuvering without deformation of body. Using the flipper apparatus as the sole source of propulsion and maneuvering forces, several underwater biorobots with rigid body have been developed to investigate the swimming performance such as efficiency and maneuvering. Based on sea turtles, Konno *et al.* developed a turtle-like submergence vehicle, whose fore fins flap for propulsion and maneuvering by combination of flapping and feathering motions [3]. In 2004 at MIT, Licht *et al.* developed a biomimetic flapping foil AUV that propels with four oscillating foils and analyzed the generation of thrust [4]. Dudek *et al.* designed a visually guided amphibious robot named AQUA at McGill University, which uses six paddles to achieve movements with six degrees of freedom [5].

In this paper, a novel turtle-like underwater robot equipped with four mechanical flippers is constructed and controlled based on central pattern generator. The robot has a number of biologically-inspired features and the contributions of this paper lie in the following. 1) The configuration of the robot is for high maneuverability, as a result, it can propel and maneuver in any direction without rotation of its main body, and execute complicated 3-D movements including ascending, submerging, rolling, and hovering by cooperative movements of four flippers. 2) The advantages of bio-gaits generated by CPG model are investigated and the influence of model parameter setting on the swimming gaits is studied. This robot shows great promise of utility in practical applications such as seabed exploration, oil-pipe leakage detection, oceanic supervision, aquatic life-form observation, military detection, and so on.

The rest of the paper is organized as follows. Section II provides the mechatronic design of the turtle-like underwater robot detailedly. In Section III, we describe the CPG model and its application to the robot. The experimental results are shown in Section IV. Finally, Section V concludes the paper.

II. CONSTRUCTION OF TURTLE-LIKE UNDERWATER ROBOT

A. General Structure of Turtle-like Robot Prototype

Inspired by softshell turtles shown in Fig. 1, a turtle-like underwater robot equipped with four mechanical flippers is developed in our laboratory. The robot assumes a modular structure including a cylindrical main body, four identical

This work was supported by National 863 Program (2006AA04Z258), 11-5 project (A2120061303), NSFC (60674050 and 60528007), and National 973 Program (2002CB312200).

W. Zhao, Y. Hu, and L. Wang are with Intelligent Control Laboratory, Department of Mechanics and Space Technologies, College of Engineering, Peking University, Beijing 100871, China. email:zhaoweijune@gmail.com.

Y. Jia is with the Seventh Research Division, Beijing University of Aeronautics and Astronautics, Beijing 100083, P. R. China.

Fig. 1. Spiny softshell turtle (*Apalone spinifera*).

flipper actuator modules and their attached wing-shaped foils. Fig. 2(a) shows the photograph of the turtle-like robot prototype and its mechanical configuration is illustrated in Fig. 2(b).

Each flipper can perform lead-lag and feathering motions, which can be controlled independently and combined to form a rowing action. The lead-lag motion actuated by the servomotor inside the main body through gear set is characterized by a posterior and anterior motion in the horizontal plane, while the feathering motion actuated by the servomotor inside flipper actuator module denotes the rotation motion of the foil. Fig. 3 illustrates the two-degree-of-freedom movements of the foil.

B. Electronics and Sensors

An embedded AT91SAM7A3-centred controller is used for controlling the servomotors to generate real-time gaits, communicating with a personal computer, and collecting the sensor data for analysis. A 2-axis accelerometer (ADXL202) is used to measure the accelerations on the pitch and roll axes. Fig. 4 presents the hardware architecture of control system for the turtle-like robot.

Finally, the basic technical parameters of this prototype are described in Table I.

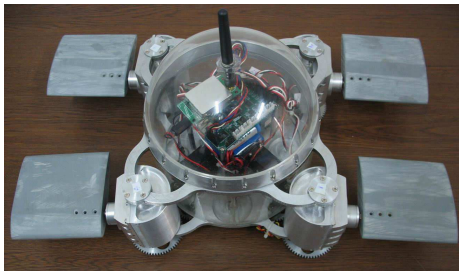

(a) Prototype

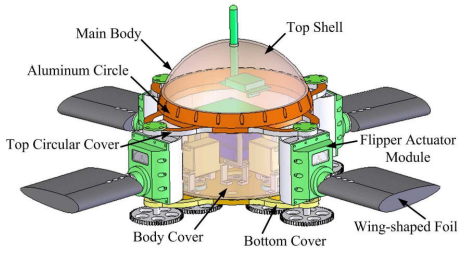

(b) General structure

Fig. 2. Prototype and general structure of turtle-like underwater robot.

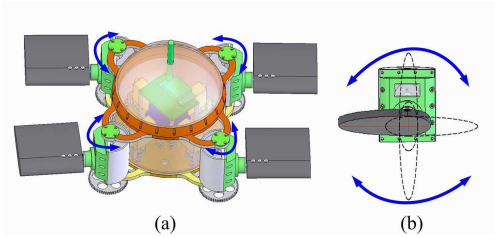

Fig. 3. Illustration of two-degree-of-freedom movements. (a) Lead-lag motion. (b) Feathering motion.

TABLE I
TECHNICAL PARAMETERS OF THE TURTLE-LIKE ROBOT PROTOTYPE.

ITEM	VALUE
Dimension (L × W × H)	∼200 mm × 200 mm × 175 mm
Weight	∼5.0 kg
Maximum oscillating frequency	4.0 Hz
Power supplying for motors	DC, 6.0 V, 2500 mAh
Power supplying for control unit	DC, 4.8 V, 2500 mAh
Microcontroller	AT91SAM7A3, 48 MHz
Operation mode	Radio Control, 444 MHz

III. CPG-BASED CONTROL

A. CPG Model

Neurobiology studies have shown that fundamental rhythmic movements in locomotion, such as walking, running, swimming, and flying, are generated by central pattern generators (CPGs) at the spinal cord level. A CPG is a neuronal circuit capable of producing rhythmic patterns of neural activity automatically and unconsciously. And CPGs are networks of neurons that can produce coordinated oscillatory signals without oscillatory inputs [6]. A typical example of CPG is found in the lamprey and has been studied extensively [7], [8]. Then CPG has been an interesting source of inspiration for motion control of robots. Ijspeert has applied CPG that produces traveling waves to an amphibious robot capable of snake-like and lamprey-like locomotion [9]. A CPG-based controller is designed for a quadruped robot capable of adaptive walking on irregular terrain by Kimura *et al.* [10].

1) Mathematical model for a singular joint: Considering neural networks and coupled nonlinear oscillators inherently have the property of limit cycle, we model each joint of the robot as a nonlinear oscillator and create a CPG by coupling

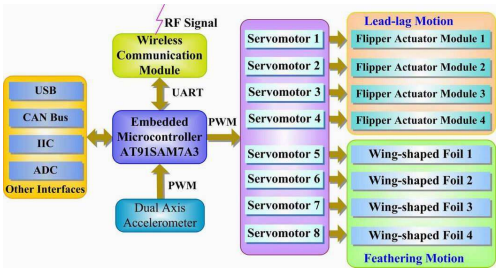

Fig. 4. Hardware architecture of control system.

the joints together. The resulting nonlinear differential equations are then solved in real time and manipulation of the CPG parameters is utilized to create different swimming gaits for the robot. Each joint of the robot actuated by servomotor can be regarded as a nonlinear oscillator taking the form of

$$\begin{cases} A\dot{\upsilon} = A\omega(\upsilon-\theta) - \upsilon(\theta^2+\upsilon^2) \\ A\dot{\theta} = A\omega(\upsilon+\theta) - \theta(\theta^2+\upsilon^2) \end{cases} \quad (1)$$

where θ denotes the desired angle of the corresponding joint of the robot, υ is another state variable, ω is a positive constant that controls both the oscillatory frequency and amplitude of the joint angle, and A is also a positive constant for adjusting only the amplitude.

Equation (1) has two particular solutions, one is zero $(0,0)$ which is an unstable fixed point, the other is a stable limit cycle which is a sinusoidal value with amplitude $\sqrt{A\omega}$ and period $2\pi/\omega$. θ will indeed converge to the particular solution $\tilde{\theta}(t) = \sqrt{A\omega}\sin(\omega t+\phi)$ from any initial conditions (θ_0, υ_0) (except zero $(0,0)$ in the phase plane), where ϕ is determined by the initial conditions. The bigger ω is, the faster the oscillator will reach its limit cycle.

The joint angle θ oscillates around $\theta = 0$ in the above nonlinear oscillator. Since the turtle-like robot can propel and maneuver in any direction by modulating the oscillatory angle's offset for each joint of mechanical flippers, we expect that the oscillator of each joint can oscillate around an arbitrary offset $\bar{\theta}$ to implement flexible motion control in 3-D space. An offset value $\bar{\theta}$ is introduced, and then (1) changes to (2) as follows:

$$\begin{cases} \Delta\theta = \theta - \bar{\theta} \\ A\dot{\upsilon} = A\omega(\upsilon-\Delta\theta) - \upsilon(\Delta\theta^2+\upsilon^2) \\ A\dot{\Delta\theta} = A\omega(\upsilon+\Delta\theta) - \Delta\theta(\Delta\theta^2+\upsilon^2) \end{cases} \quad (2)$$

The solution will converge to $\tilde{\theta}(t) = \bar{\theta} + \sqrt{A\omega}\sin(\omega t+\phi)$ in (2).

2) Coupling joints together: The above nonlinear oscillator illustrates a singular joint's behavior property. The gait pattern can be generated by coupling joints together, so a coupling term should be added to (2) in the following way:

$$\begin{cases} \Delta\theta_i = \theta_i - \bar{\theta}_i \\ A_i\dot{\upsilon}_i = A_i\omega(\upsilon_i-\Delta\theta_i) - \upsilon_i(\Delta\theta_i^2+\upsilon_i^2) + A_i\sum_j(a_{ij}\theta_j + b_{ij}\upsilon_j) \\ A_i\dot{\Delta\theta}_i = A_i\omega(\upsilon_i+\Delta\theta_i) - \Delta\theta_i(\Delta\theta_i^2+\upsilon_i^2) \end{cases} \quad (3)$$

where θ_i denotes the desired angle of the i-th joint of the robot, $\bar{\theta}_i$ indicates the angular offset added to the i-th joint, a_{ij} and b_{ij} are the connection weights to define the coupling between the i-th and the j-th joints (i.e. the influence that the j-th joint has on the i-th one). Cooperative movements can be obtained by modulating the phase-lag or phase-lead relationship between coupled joins, which is determined by the coupling coefficients a_{ij} and b_{ij}.

In mathematics and computational science, the Euler method, named after Leonhard Euler, is a numerical procedure for solving ordinary differential equations. In Euler method, $[\upsilon(k+1)-\upsilon(k)]/T$ is used instead of $\dot{\upsilon}$, so the differential equations are transformed into difference equations.

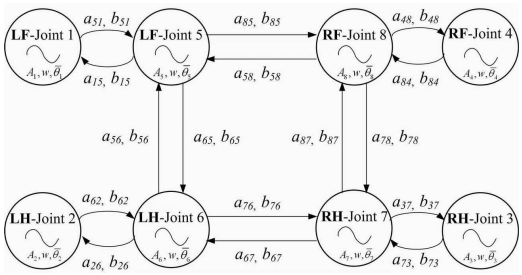

Fig. 5. CPG network for the turtle-like robot. The joints 1, 2, 3, 4 correspond to lead-lag motion, while joints 5, 6, 7, 8 correspond to feathering motion. L, R, F and H denote the left, right, fore or hind flippers, respectively.

As a result, the differential equations in (3) are then changed to difference equations using Euler method in the following way:

$$\begin{cases} \Delta\theta_i(k) = \theta_i(k) - \bar{\theta}_i \\ A_i\frac{\upsilon_i(k+1)-\upsilon_i(k)}{T} = A_i\omega(\upsilon_i(k)-\Delta\theta_i(k)) - \upsilon_i(k)(\Delta\theta_i^2(k)+\upsilon_i^2(k)) \\ \qquad +A_i\sum_j(a_{ij}\theta_j(k)+b_{ij}\upsilon_j(k)) \\ A_i\frac{\Delta\theta_i(k+1)-\Delta\theta_i(k)}{T} = A_i\omega(\upsilon_i(k)+\Delta\theta_i(k)) - \Delta\theta_i(k)(\Delta\theta_i^2(k)+\upsilon_i^2(k)) \end{cases} \quad (4)$$

where $\theta_i(k)$ represents the i-th joint's angle at the k-th time, T denotes the step size of time, and the initial conditions can be set as $\theta_i(0) = 0$, $\upsilon_i(0) \neq 0$. Through recursive algorithm, $\theta_i(k)$ can be calculated from (4) online.

B. CPG-based Method

The control for turtle-like robot is based on the above CPG model that generates the rhythmic movements for realtime gait generation. Since the robot is composed of four mechanical flippers with two joints each, the CPG model of (4) can be applied to an eight-joint system established for the turtle-like robot, as illustrated in Fig. 5. By connecting the CPG of each joint, CPGs are mutually entrained and oscillate in the same frequency and with a fixed phase difference. This mutual entrainment between the CPGs of the flippers results in a swimming gait.

As observed from (4), a parametric vector **E**=$\{A_1 \sim A_8, \omega, \bar{\theta}_1 \sim \bar{\theta}_8, a_{ij}, b_{ij}\}$ regulating the swimming gaits of the turtle-like robot can be summarized. The setting of these parameters is to generate a proper swimming pattern according to turtle swimming character. In the CPG model, $\bar{\theta}_1 \sim \bar{\theta}_8$ determine the propulsive orientation of the robot, the connection weights a_{ij}, b_{ij} determine the phase difference $\Delta\Phi_{ij}$ between connected joins, $A_1 \sim A_8$ determine small or large amplitude swimming modes, and ω determines the oscillatory frequency. Based on the proposed CPG model, several swimming patterns and actions will be described next, and the advantages of bio-gaits, the influence of parameter setting on the swimming gaits will be given detailedly in simulations.

1) Typical swimming patterns: Considering the parameter setting in swimming patterns design, the following points are proposed beforehand:

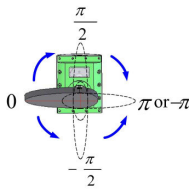

Fig. 6. Illustration of angular offset for a foil.

- The angular offset $\bar{\theta}_i$ added to feathering joints ($i = 5 \sim 8$) can range from $-\pi$ rad to π rad, as illustrated in Fig. 6.
- In the case of $A_i = 0$, whatever value ω, a_{ij}, and b_{ij} are set to, the solution will converge to $\tilde{\theta}_i(t) = \bar{\theta}_i$ in (4).
- In the case of $A_i \neq 0$, the oscillatory amplitude for joint i is approximately $\sqrt{A_i}\omega$.

Based upon the joints used, the swimming can be classified into two basic modes: **FJ** (feathering joints) mode and **LFJ** (combination of lead-lag and feathering joints) mode. By modulating the oscillatory angle's offset for each foil, the turtle-like robot can accomplish complex movements in 3-D space. By cooperative movements of four symmetrical flippers combining lead-lag motion and feathering motion, the turtle-like robot can propel and maneuver in any direction without any rotation of its main body. As illustrated in Fig. 7, several typical swimming patterns with two modes have been designed and implemented on the robot by adopting different CPG model parameters.

2) Rowing action: Rowing action, by coupling lead-lag motion and feathering motion together, can also perform forward swimming, backward swimming, and turning in the horizontal plane. In rowing action, the foils of our robot are brought "forward almost edgewise and back broadside" [11]. A sequence of rowing action is illustrated in Fig. 8. Rowing involves anteroposterior movements and rotations of the foils. The oscillations of lead-lag joint and feathering joint of one flipper are of the same frequency. The setting of CPG model parameters in rowing action will be studied via simulations.

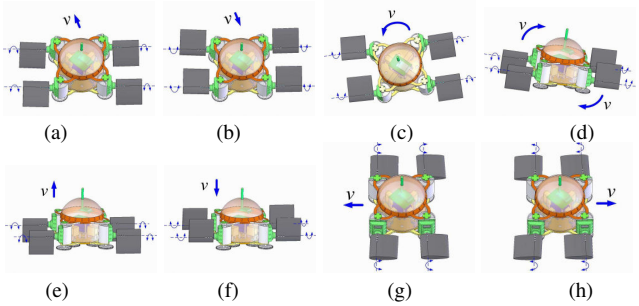

Fig. 7. Illustrations of eight typical swimming patterns designed for turtle-like underwater robot. (a) FJ forward swimming. (b) FJ backward swimming. (c) FJ turning. (d) FJ rolling. (e) FJ ascending. (f) FJ submerging. (g) LFJ Leftward swimming. (h) LFJ rightward swimming.

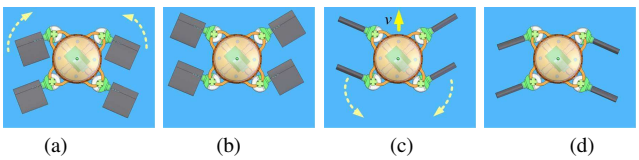

Fig. 8. A sequence of rowing action. Swimming forward edgewise [from (a) to (b)] and swimming back broadside [from (c) to (d)].

C. Simulations

1) Study of characteristics of CPG-based bio-gait generation: We conducted a series of simulation experiments to demonstrate the coordination, swiftness, adaptation, and diversity of the proposed CPG-based method. First, taking rolling for example, the ability of the CPG-based method was tested to show elegant and smooth transitions between swimming gaits, and enhanced ability to cope with transient perturbations due to nonlinear characteristic.

An example of such solutions that generate rolling movement is given in Fig. 9, where $\theta_5(t) \sim \theta_8(t)$ represent oscillatory angles of all four foils of the robot, and the CPG model parameters are set as $A_1 = A_2 = A_3 = A_4 = 0$, $\bar{\theta}_1 = \bar{\theta}_2 = \bar{\theta}_3 = \bar{\theta}_4 = 0$, $\omega = 4\pi$, $A_5 = A_6 = A_7 = A_8 = 32$ (S.t.$\sqrt{A_i}\omega \approx 20^\circ, i = 5,6,7,8$), $\bar{\theta}_5 = \bar{\theta}_6 = -\pi/2$, $\bar{\theta}_7 = \bar{\theta}_8 = \pi/2$, $a_{ij} = b_{ij} = 0$ $(i,j = 1,2,3,4,5,6,7,8)$, $t = 0 \sim 2.5$ s. In particular, the frequency and amplitude of all foils are modulated by changing the parameters $\omega \to 8\pi, A_i \to 36$ $(i = 5,6,7,8)$ at time $t = 1.5$ s. As a consequence, the oscillatory frequency (almost $\omega/2\pi$) rises approximately from 2 Hz to 4 Hz and the oscillatory amplitude for i-th joint (nearly $\sqrt{A_i}\omega, i = 5,6,7,8$) is approximately modulated from 20° to 30° at the same time $t = 1.5$ s. As shown in Fig. 9, the oscillation of each foil can smoothly and easily adapt to the abrupt change of oscillatory frequency and oscillatory amplitude determined by CPG model parameters. As a result, the adjustment of the speed of the robot can be smooth and easy.

Furthermore, nonlinear oscillators of CPG model have enhanced ability to cope with transient perturbations due to nonlinear characteristic. When correctly coupled, the oscillators in a circle will produce stable limit cycle behaviors after any type of transient perturbation. Fig. 10 illustrates this property. At a given time, random perturbations are applied to all oscillatory angles of the foils $\theta_5 \sim \theta_8$. After a short transitory period, the system quickly and smoothly returns to the original swimming gait.

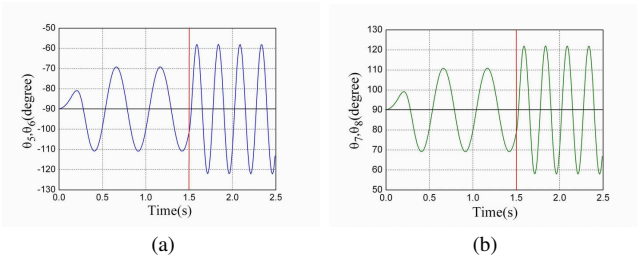

Fig. 9. Modulation of both the oscillatory frequency and amplitude of the foils by changing the CPG model parameters at time $t = 1.5$ s.

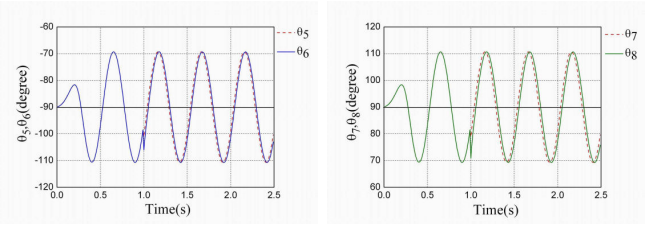

(a) (b)

Fig. 10. Random perturbation of the oscillatory angles of the foils at time $t = 1$ s.

In conclusion, due to online calculation and nonlinear characteristic, CPG-based method possesses a range of advantages: (1) the oscillation of each joint can smoothly and easily adapt to the abrupt change of oscillatory frequency and oscillatory amplitude determined by CPG model parameters (see Fig. 9), and (2) enhanced ability to cope with transient perturbations (see Fig. 10). Hence this CPG-based method provides good adaptation to both modifications of the control parameter and random perturbations in the environment.

2) Study of a flipper system with two coupled nonlinear oscillators in rowing action: Since the behaviors of the four mechanical flippers in rowing action are almost the same, a system is investigated to get an idea of how interconnected oscillators in a same flipper behave, especially how the phase relation between them is determined by the connection weights. Fig. 11 shows the quarter-CPG we are going to study. In this system, the CPG model parameters include A_i, A_{i+4}, ω, $\bar{\theta}_i$, $\bar{\theta}_{i+4}$, $a_{i+4,i}$, $b_{i+4,i}$, $a_{i,i+4}$, $b_{i,i+4}$.

In rowing action, the phase difference $\Delta\phi_{i,i+4}$ between lead-lag joint i ($i = 1,2,3,4$) and feathering joint $i+4$ will determine different types of rowing strokes. To perform "forward almost edgewise and back broadside", the rule of setting these model parameters to produce a rowing stroke is given by

$$\Delta\phi_{i,i+4} \in [-\pi/4, \pi/4] \qquad i = 1,2,3,4 \tag{5}$$

As mentioned before, the amplitude and the frequency of each oscillator can be easily controlled through A_i and ω. Besides, in CPG network, it is also crucial to control the phase relation between coupled oscillators, which will be carried out by the connections between the oscillators. After the system starts the phase of each oscillator first defined by its initial conditions θ_0 and υ_0, the connections will quickly force a particular phase relation. Through simulations on CPG model (4), the influence of the connection weights on the oscillations of coupled joints has been investigated. On the other hand, based on the simulation results that give the dependence of phase difference on connection weights, the

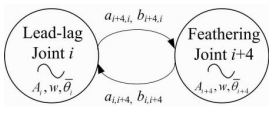

Fig. 11. A flipper system made of two nonlinear oscillators linked together.

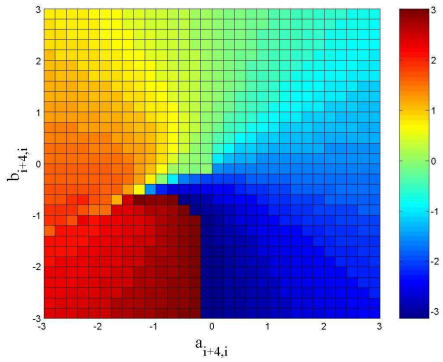

Fig. 12. Phase difference $\Delta\Phi_{i,i+4}$ (rad) with $a_{i,i+4} = 0$ and $b_{i,i+4} = 0$.

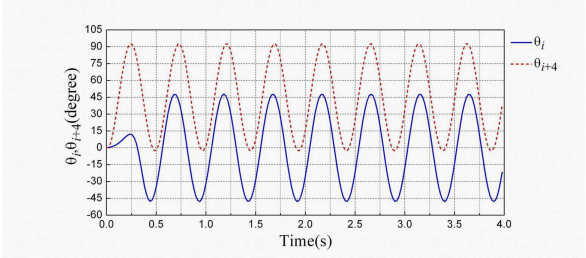

Fig. 13. Oscillatory angles of lead-lag joint and feathering joint of a same flipper based on the CPG model during rowing action.

CPG model parameters can be chosen obeying the rule in (5).

The following example will illustrate how the phase difference $\Delta\phi$ between the two coupled joints is determined by the connection weights a and b by some simulation results. For simplicity, we supposed that only the feathering joint can receive a signal from its lead-lag one, i.e., $a_{i,i+4}$ and $b_{i,i+4}$ were set to 0. All of the parameters were set as follows: $\omega = 4\pi$, $A_i = A_{i+4} = 161$ (S.t.$\sqrt{A_i\omega} = \sqrt{A_{i+4}\omega} \approx 45°$), $\bar{\theta}_i = 0$, $\bar{\theta}_{i+4} = \pi/4$, $a_{i,i+4} = b_{i,i+4} = 0$, only $a_{i+4,i}$ and $b_{i+4,i}$ were free variables. In the case of $a_{i+4,i} = 0$ and $b_{i+4,i} = 0$, there is no coupling term and the two joints of a same flipper both run freely with phase differences $\Delta\Phi_{i,i+4} = 0$, which exactly fits the condition in rule (5). As a result, the values of $a_{i+4,i}$ and $b_{i+4,i}$ could be set around 0 for simulating. In this example, the values of $a_{i+4,i}$ and $b_{i+4,i}$ were iteratively changed between -3 and 3. The simulation results in this case are given in Fig. 12, stating how the phase difference $\Delta\Phi_{i,i+4}$ changes with the modification of $a_{i+4,i}$ and $b_{i+4,i}$. It can be concluded that the phase difference $\Delta\Phi_{i,i+4}$ depends on the quadrant in which the point ($a_{i+4,i}$, $b_{i+4,i}$) locates regularly. The plane is approximately split into two symmetric areas by the line $a_{i+4,i} = 0$. In the area where $a_{i+4,i} > 0$, the oscillation of the lead-lag joint lags that of the corresponding feathering joint in phase, while phase-lead relation happens in the area of $a_{i+4,i} < 0$. Observed from the figure, the phase difference $\Delta\Phi_{i,i+4}$ satisfies the rule in (5) stably in the areas of $b_{i+4,i} > a_{i+4,i} > 0$ and $b_{i+4,i} > -a_{i+4,i} > 0$.

Considering the rule and the simulation results, a set of solutions that generate rowing action have been obtained in our simulation and experiments. An example of such solu-

tions $\theta_i(t)$ and $\theta_{i+4}(t)$ that respectively represent oscillatory angles of lead-lag joint and feathering joint of a same flipper is illustrated in Fig. 13, where $\omega = 4\pi$, $A_i = A_{i+4} = 161$ (S.t.$\sqrt{A_i\omega} = \sqrt{A_{i+4}\omega} \approx 45°$), $\bar{\theta}_i = 0$, $\bar{\theta}_{i+4} = \pi/4$, $a_{i+4,i} = -0.5$, $b_{i+4,i} = 0.6$, $a_{i,i+4} = 0$, $b_{i,i+4} = 0$, and $t = 0 \sim 4$ s. As shown in this figure, the phase relationship between the two coupled nonlinear oscillators of each flipper means to produce an appropriate type of rowing motion.

IV. EXPERIMENTS AND RESULTS

A. Evaluation of Swimming Speed

For FJ forward swimming pattern, the average linear speed is tested by varying the frequency and amplitude of foil oscillations. Steady-state speed was measured at different levels of frequencies and amplitudes of all foils. Three groups of foil oscillatory amplitudes are employed while the frequency is varied in each case. As illustrated in Fig. 14, the swimming speed increases with the oscillatory amplitude until the peak value on amplitude of 30° and almost linearly with the oscillatory frequency. The swimming speed decreases with the enhancement of the amplitude after reaching its peak value because the oscillations become so large as to generate braking waves. Overall, the robot can swim up to the speed of 19.8 cm/s at a frequency of 4 Hz and amplitude of 30°.

B. Testing of Swimming Patterns Sequentially

The ability of the CPG-based method was tested to produce different types of swimming patterns presented above. For convenience of clearly observing swimming patterns in 3-D space, the tests of sequential patterns were conducted in a transparent water tank. Fig. 15 presents the variations of oscillatory angles of eight joints when executing a sequence of typical swimming patterns. The turtle-like robot can change its postures from one pattern to another smoothly. The sequentially executed swimming patterns include FJ forward swimming ($t \leq 5s$), FJ backward swimming ($5s < t \leq 10s$), FJ turning ($10s < t \leq 15s$), FJ ascending ($15s < t \leq 20s$), FJ submerging ($20s < t \leq 25s$), FJ rolling ($25s < t \leq 30s$), LFJ leftward swimming ($30s < t \leq 35s$), and LFJ rightward swimming ($35s < t \leq 40s$).

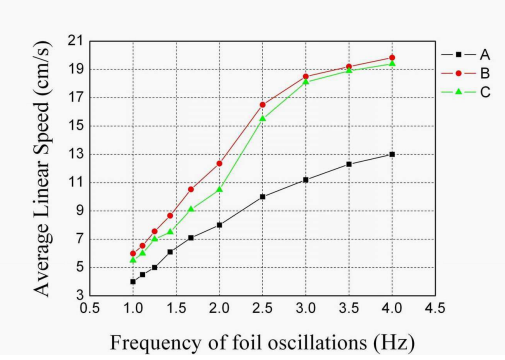

Fig. 14. Average linear speed in FJ forward swimming with different frequencies and amplitudes. The amplitudes used in each case are: A=$\{A_i = 400/\omega\}$ (S.t.$\sqrt{A_i\omega} = 20°$), B=$\{A_i = 900/\omega\}$ (S.t.$\sqrt{A_i\omega} = 30°$), C=$\{A_i = 1600/\omega\}$ (S.t.$\sqrt{A_i\omega} = 40°$), $i = 5,6,7,8$.

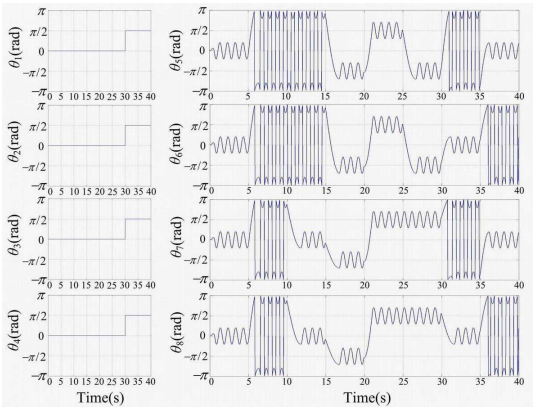

Fig. 15. Variations of oscillatory angles of eight joints when executing a sequence of typical swimming patterns.

V. CONCLUSIONS

In this paper, a flipper propelled turtle-like underwater robot was constructed and controlled based on central pattern generator. The cooperative movements of four symmetrical flippers could generate propulsion and maneuvering in any direction without any rotation of the main body. The advantages of CPG-based gait generation were proposed and demonstrated via simulations. The experimental results demonstrated high maneuverability of the robot and confirmed the effectiveness of the proposed method.

REFERENCES

[1] M. S. Triantafyllou and G. S. Triantafyllou, "An efficient swimming machine", *Sci. Amer.*, vol. 272, no. 3, 1995, pp. 64-70.

[2] D. Barrett, M. Grosenbaugh, M. Triantafyllou, "The optimal control of a flexible hull robotic undersea vehicle propelled by an oscillating foil", in *Proc. IEEE AUV Symposium*, 1996, pp. 1-9.

[3] A. Konno, T. Furuya, A. Mizuno, K. Hishinuma, K. Hirata, and M. Kawada, "Development of turtle-like submergence vehicle", in *Proc. Int. Symp. Marine Engineering*, 2005, pp. 1-5.

[4] S. Licht, V. Polidoro, M. Flores, F. Hover, M. Triantafyllou, "Design and projected performance of a flapping foil AUV", *IEEE J. Oceanic Eng.*, vol. 29, 2004, pp. 786-794.

[5] G. Dudek, M. Jenkin, C. Prahacs, A. Hogue, J. Sattar, P. Giguere, A. German, H. Liu, S. Saunderson, A. Ripsman, S. Simhon, L.-A. Torres, E. Milios, P. Zhang, I. Rekletis, "A visually guided swimming robot", in *Proc. IEEE/RSJ Int. Conf. Intelligent Rob. and Sys.*, 2005, pp. 3604-3609.

[6] F. Delcomyn, "Neural basis for rhythmic behaviour in animals", *Science*, vol. 210, 1980, pp. 492-498.

[7] J. Buchanan, S. Grillner, "Newly identified 'glutamate interneurons' and their role in locomotion in the lamprey spinal cord", *Science*, vol. 236, 1987, pp. 312-314.

[8] S. Grillner, P. Wallen, L. Brodin, "Neuronal network generating locomotor behavior in lamprey: Circuitry, transmitters, membrane properties, and simulation", *Annual Review of Neuroscience*, vol. 14, 1991, pp. 169-199.

[9] A. Crespi, A. Badertscher, A. Guignard, and A. J. Ijspeert, "Amphibot I: an amphibious snake-like robot", *Robot. Auton. Syst.*, vol. 50, 2005, pp. 163-175.

[10] H. Kimura, Y. Fukuoka, and K. Konaga, "Adaptive dynamic walking of a quadruped robot using a neural system model", *Adv. Robot.*, vol. 15, 2001, pp. 859-876.

[11] M. W. Westneat, and J. A. Walker, "Applied aspects of mechanical design, behavior, and performance of pectoral fin swimming in fishes", in *Proceedings of the Conference on Unmanned, Untethered Submersible Technology. Autonomous Underwater Systems Institute*, Durham, N. H., 1997, pp. 1-14.